JOURNAL OF MATERIALS SCIENCE **36** (2001) 3453–3459

Reactive ion etching of diamond in CF_4, O_2, O_2 and Ar-based mixtures

P. W. LEECH
CSIRO Division of Manufacturing Science and Technology, Victoria, Australia
E-mail: patrick.leech@cmst.csiro.au

G. K. REEVES, A. HOLLAND
School of Electrical and Computer Systems Engineering, R.M.I.T. University, Victoria, Australia

The reactive ion etching of diamond in O_2, CF_4/O_2, CHF_3/O_2, O_2/Ar discharges has been examined as a function of bias voltage, flow rate and composition of the gas mixtures. Etching in O_2 and O_2/Ar plasmas (with flow ratio of $O_2/Ar \geq 25\%$) was characterised by a high etch rate (∼35 nm/min) and an increase in surface roughness with rising bias voltage. The CF_4/O_2 plasmas also produced a high etch rate (∼50 nm/min) but with only minor dependence of roughness on bias voltage. In comparison, the O_2/Ar (with O_2/Ar flow ratio $<25\%$) and CHF_3/O_2 plasmas resulted in a low etch rate (7–10 nm/min). The high and low rate regimes were identified as ionenhanced chemical etching and physical sputtering respectively. Etching in the O_2/Ar plasmas has been attributed to a combination of the two processes dependent on the O_2 content. © *2001 Kluwer Academic Publishers*

1. Introduction

The unique properties of diamond films have enabled the design of high performance devices in microelectronics and optics. Recent examples of designs incorporating a diamond film have included high power transistors, surface acoustic wave detectors at GHz frequencies, light emitting diodes and elevated temperature integrated circuits [1]. Films of diamond suitable for the fabrication of these devices have been grown by homoepitaxial methods while large-area wafers of diamond-on-silicon have become available through chemical vapour deposition (CVD) [2]. However, one of the major issues in the realisation of active devices has remained the ability to lithographically pattern the film by etching. Several methods of etching of diamond have been reported including reactive ion etching [3–10], irradiation with a focused ion [11, 12] or laser beam [13] and synchrotron excited radiation [14]. Of these, the reactive ion etching (RIE) of diamond has the inherent advantages of compatibility with lithographic techniques and the ability to select from a range of reactants.

Plasmas based on pure O_2 have produced moderately high yet erratic rates of reactive ion etching of diamond although accompanied by an increase in roughness of the surface [3, 4, 6, 7, 9]. The addition of Ar has resulted in a greater uniformity and reproducability than in pure O_2 [4, 9]. In contrast, the etching of diamond in SF_6 [6] and CF_4 [10] plasmas has produced a rounding of the peaks on the surface of the diamond but without a decrease in overall roughness. H_2 and mixtures of H_2/O_2 and H_2/Ar have been shown to polish the surface of diamond although at an extremely slow rate [5, 8]. But any comparison between these trends has been restricted by the use of different types of etch system, varying conditions of etching and crystal orientation. The present paper has directly compared for the first time the reactive ion etching of CVD grown diamond in a range of plasmas of potentially reactive plasmas (O_2, CF_4/O_2, CHF_3/O_2, O_2/Ar) and in the inert noble Ar. The details of etch rate and surface morphology have been characterised as a function of the parameters of the RIE system and interpreted in terms of the mechanism of etching.

2. Experimental details

The diamond film used in this study was grown by microwave plasma enhanced chemical vapour deposition (PECVD) on a silicon wafer with a diameter of 76 mm. The thickness of the deposited film was 2.6 μm. Analysis by X-ray diffraction has revealed a dominant peak at $2\theta = 44°$ corresponding to a $\langle 111 \rangle$ oriented surface with a FWHM of 0.2°.

The dry etching was performed in a commercial STS320 system with RF powering at 13.56 MHz. The cathode in this system was 37 cm in diameter and was continuously cooled to a temperature of 20 °C. A base pressure in the chamber of $\sim 1 \times 10^{-6}$ torr was maintained by a turbomolecular pump backed by a rotary pump. Prior to each experiment, the electronic grade gases of either O_2, Ar, O_2/Ar, CF_4/O_2 or CHF_3/O_2 were introduced into the reaction chamber by means of mass flow controllers. These gases were mixed prior

to entering the chamber through a shower plate in the top electrode. The etch rate of the diamond film in each of the plasmas was measured as a function of RF power from 80 to 430 W (corresponding to bias voltages of −280 V to −560 V). This series of experiments included varying the ratios of the O_2/Ar mixture. The compositions examined were O_2 (45 sccm), O_2 (35 sccm)/Ar (10 sccm), O_2 (25 sccm)/Ar (20 sccm), O_2 (10 sccm)/Ar (35 sccm) and pure Ar (45 sccm). The etch rate was also measured versus the flow rate of the O_2, CF_4/O_2 or Ar gases (8 to 50 sccm) at 250 W and 50 mTorr. In the CF_4/O_2 and CHF_3/O_2 plasmas, the presence of a minor amount of O_2 (1 sccm) was included to reduce the formation of fluorocarbon during etching.

Etch steps were formed on the surface of the diamond film by masking with a section of alumina wafer. The etch depth in the diamond film was measured using a Dektak stylus profilometer with an average of 5 scans performed after each experiment. In addition, a selection of features on the surfaces of the as-grown and etched samples was examined by atomic force microscopy (AFM) using a Digital Instruments Dimension 3100 Nanoscope.

3. Results and discussion

During etching in the plasmas, the etch depth was measured as a linear function of time for periods up to 45 minutes indicating a steady state removal of etch products from the surface. The constant etch rate also coincided with a constant value of the bias voltage, V_b during these tests.

Fig. 1 shows the dependence of etch rate of the diamond film on the square root of bias voltage for O_2, Ar, O_2/Ar, CF_4/O_2 and CHF_3/O_2 plasmas. Previously, Steinbruchel *et al.* [16] have shown that reactive ion etching of a wide range of materials occurred by a process of either physical sputtering or ion-enhanced chemical etching. In both types of process, the etch yield Y(E) was described by the expression:

$$\mathrm{Y(E)} = A\left(E_i^{1/2} - E_{\mathrm{th}}^{1/2}\right) \qquad (1)$$

where E_i = ion energy and A and E_{th} were constants representing the slope and threshold energy of etching respectively. The magnitude of E_i was shown as directly proportional to the d-c bias voltage, V_b, induced at the cathode by the application of r-f power [17].

In Fig. 1, a least squares fit of Equation i to the data has also shown a linear dependence of the etch rate on $V_b^{1/2}$. A summary of the values of A and etch rate at a bias voltage of $V_b = 576$ V has been given in Table I for each of the gases or mixtures. In Fig. 1, the highest etch rates were obtained with the CF_4 (44 sccm)/O_2 (1 sccm) and pure O_2 plasmas. A greater dependence of etch rate on $V_b^{1/2}$ was evident for the CF_4/O_2 ($A = 4.87$) than for the CHF_3/O_2 ($A = 0.98$). For etching in the O_2 and O_2 (35 sccm)/Ar (10 sccm) plasmas, the slope of etch rate versus $V_b^{1/2}$ steadily increased with proportion of O_2 in the plasma. As a measure of this change in etch rate with O_2/Ar ratio, the value of the slope constant in Equation i increased from $A = 0.26$ in pure Ar to $A = 3.57$ in pure O_2. The etch rate in Ar remained in the range ∼5–7 nm/min and was only weakly dependent on $V_b^{1/2}$. As an indication of the quality of fit of the data to this form of equation, the value of r^2 (the square of the correlation coefficient) was calculated from each

TABLE I Values of slope constant, A, and etch rate at $V_b = 576$ V (50 mTorr)

	A (nm/min/$V^{1/2}$)	Etch Rate (nm/min) at $V^{1/2} = 576$ V
CF_4/O_2	4.87	37.5
CHF_3/O_2	0.98	10
O_2	2.72	33
O_2 (35 sccm)/Ar (10 sccm)	1.95	28.3
O_2 (25 sccm)/Ar (20 sccm)	1.08	20
O_2 (10 sccm)/Ar (35 sccm)	1.01	12.5
Ar	1.01	8

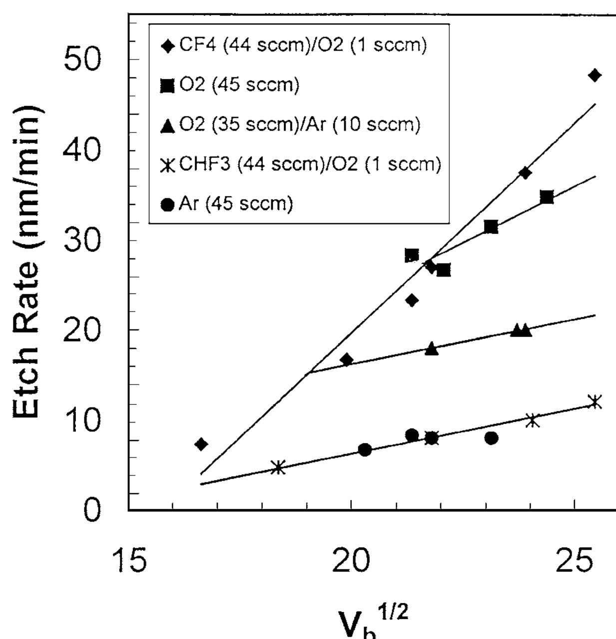

Figure 1 Etch rate of diamond versus $V_b^{1/2}$ at 45 sccm and 50 mT.

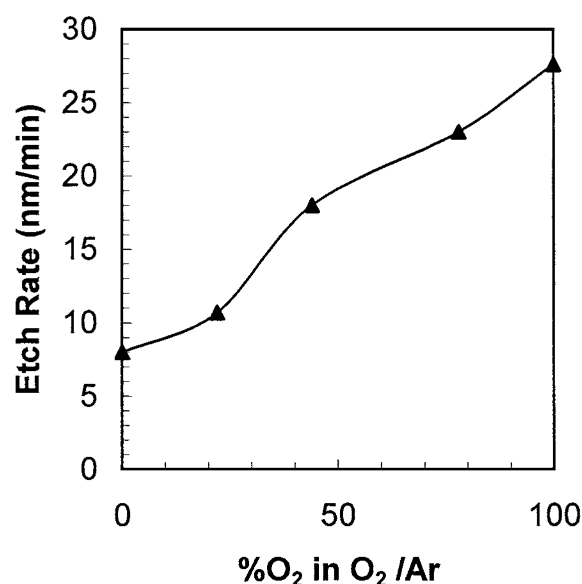

Figure 2 Etch rate versus proportion of O_2 in O_2/Ar plasmas, 250 W, 50 mT.

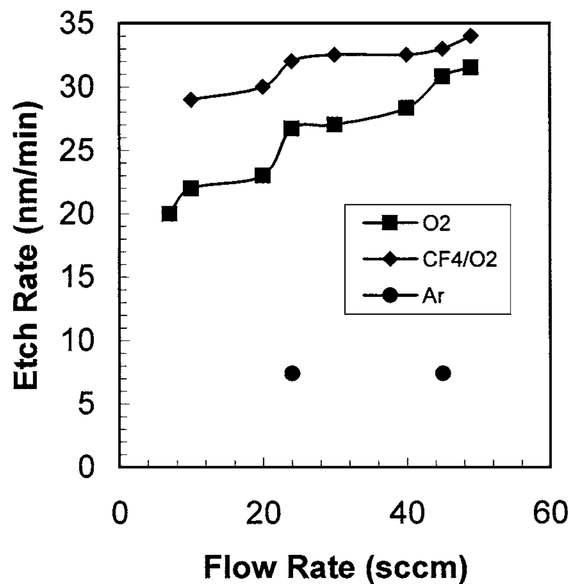

Figure 3 Etch rate versus flow rate in O_2, CF_4/O_2 and Ar plasmas.

plot. The measured value of r^2 was in the range from 0.95 for CF_4 (44 sccm)/O_2 to 0.99 for O_2, indicating a good quality of fit.

The dependence of etch rate on the proportion of O_2 in O_2/Ar plasmas at a constant r-f power of 250 W has also been plotted in Fig. 2. In these experiments, the total flow rate of O_2 plus Ar was held constant at 45 sccm with the chamber pressure at 50 mTorr. In Fig. 2, the etch rate steadily increased with rising proportion of O_2 from 0 to 100% O_2. At the limits of this range, the ratio of etch rates of pure O_2 to pure Ar plasmas was in the ratio of 4 : 1. In Fig. 3, the etch rate has been plotted as a function of the flow rate of a) O_2 gas and b) CF_4 in a CF_4/O_2 (1 sccm) plasma. The power was constant at 250 W and pressure at 50 mTorr. Both plots have shown a continuous rise in etch rate with increasing flow rate although the O_2 produced a stronger effect than the CF_4/O_2 plasma. Etch rate in the Ar plasma was essentially independent of the flow rate with a value of etch rate of 7–9 nm/min (Fig. 3).

0.5μm

μm

1 2 3 4 5

(a)

Figure 4 AFM images of a) unetched diamond and etched in b) O_2, c) CF_4/O_2 and d) O_2/Ar plasmas *(Continued)*.

Typical images obtained by AFM of the surfaces of a) as-grown diamond and after etching in b) O_2, c) CF_4/O_2 and d) O_2/Ar plasmas have been illustrated in Fig. 4a–d. The images of the unetched surfaces revealed the individual grains or facets formed during the growth process with an average diameter of 2-3 μm with R_a (average roughness) in the range of 2-3 nm. Also evident within the grains was a much finer structure with lateral dimensions of $\sim$0.1 μm. The effect of etching in an O_2 plasma was to increase the roughness of the surface with the formation of a pattern of rounded nodules of spacing $\sim$0.1–0.3 μm (Fig. 4b). For these surfaces etched in an O_2 plasma, Fig. 5 shows that R_a increased steeply to a value of 15 nm with rising r-f power above $\sim$250 W. Etch experiments using the O_2 (35 sccm)/Ar (10 sccm) and O_2 (20 sccm)/Ar (25 sccm) plasmas produced a R_a which was similar to the pure O_2. However, when the O_2 content was reduced to a level of $\leq$10 sccm in a mixture of O_2 (10 sccm)/Ar (35 sccm), the value of R_a decreased slightly with rising power as seen in Fig. 5, thereby effectively acting to polish the surface of the diamond. An AFM image of a surface etched in O_2 (10 sccm)/Ar (35 sccm), in Fig. 4c has illustrated the polishing effect. The AFM images of the surfaces etched in the CF_4 /O_2 plasmas in Fig. 4d have suggested a smoothing of the peaks in the original faceted structure but with the outline of the grains still present. A minor increase in roughness occurred with rising power but of a much lesser magnitude than occurred in the O_2-rich plasmas (Fig. 5).

These results have been interpreted in terms of the two recognised processes of ion-enhanced chemical etching and physical sputter etching. Both of the processes have been previously shown to exhibit a direct dependence of etch rate on $E^{1/2}$ (and hence $V_b^{1/2}$) although the etch rates and slope constant, A, for ion-enhanced chemical etching were significantly higher than for physical sputtering [18]. In the present results,

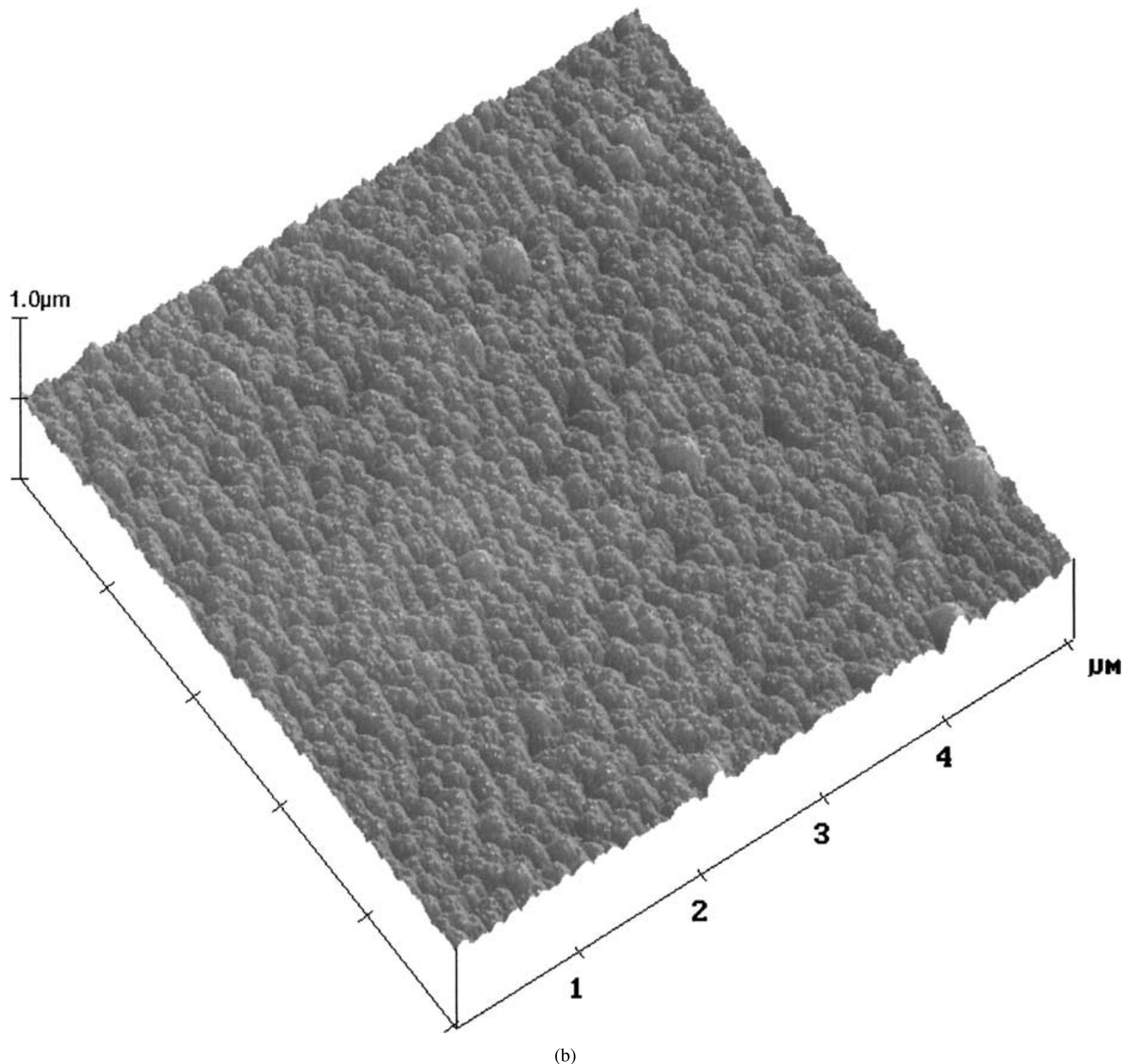

(b)

Figure 4 (Continued).

the etching of the diamond film in the O_2, the O_2 (35 sccm)/Ar (10 sccm), O_2 (25 sccm)/Ar (20 sccm) and CF_4/O_2 plasmas has been attributed to an ion-enhanced chemical reaction. In these plasmas, the etching was characterised by moderately high values of etch rate and slope constant, A, together with a dependence on flow rate. In the O_2 plasmas, the etching has been attributed to a dissociation into O radicals [19] accompanied by the formation of volatile etch products of CO and CO_2. On the surfaces during etching in the O_2 plasmas, the rounded, nodular structures (0.1–0.3 μm) were evidently a type of preferential attack of the diamond. The lateral scale of these nodular structures was similar to the fine structure on the as-grown surfaces, indicating that the fine protrusions may have etched preferentially around their base to produce nodules. Bachmann *et al.* have shown an increased sputter rate at grain boundaries of CVD diamond due to an enhanced distribution of graphite in these regions [20]. In CF_4/O_2 plasmas, the main chemical reactants of C and CF_n^+ have been previously reported to adhere to the surface of the diamond leading to highly volatile etch products [10]. In this regime, the effect of flow rate on etch rate (Fig. 3) has been attributed to an increased supply of ions for potential reaction. The effect of flow rate of the gases in increasing etch rate (Fig. 5) was evidently unrelated to changes in bias voltage. As flow rates in the CF_4/O_2 plasmas increased from 10 to 49 sccm, the bias voltage decreased from 490 to 456 V, the opposite sense to that required for the increase in etch rate. In the O_2 plasmas, the bias voltage was constant with variation in flow rate from 7–45 sccm.

In the Ar and Ar (35 sccm)/O_2 (10 sccm) plasmas, the comparatively low etch rate (7–9 nm/min), the low value of the constant, A (Table I) and insensitivity to flow rate have indicated a regime of sputter etching. A further indication of sputter etching was the similarity between these etch rates and the process of physical sputtering of diamond by an Ar ion gun which was reported to give a maximum etch rate of 11.1 nm/min at 1 KeV (60° incidence) [13]. The lower etch rate in the present results was consistent with a lesser ion energy (290–570 eV) using RIE than obtained by ion milling (1,000 eV). The surfaces formed by Ar ion etching have

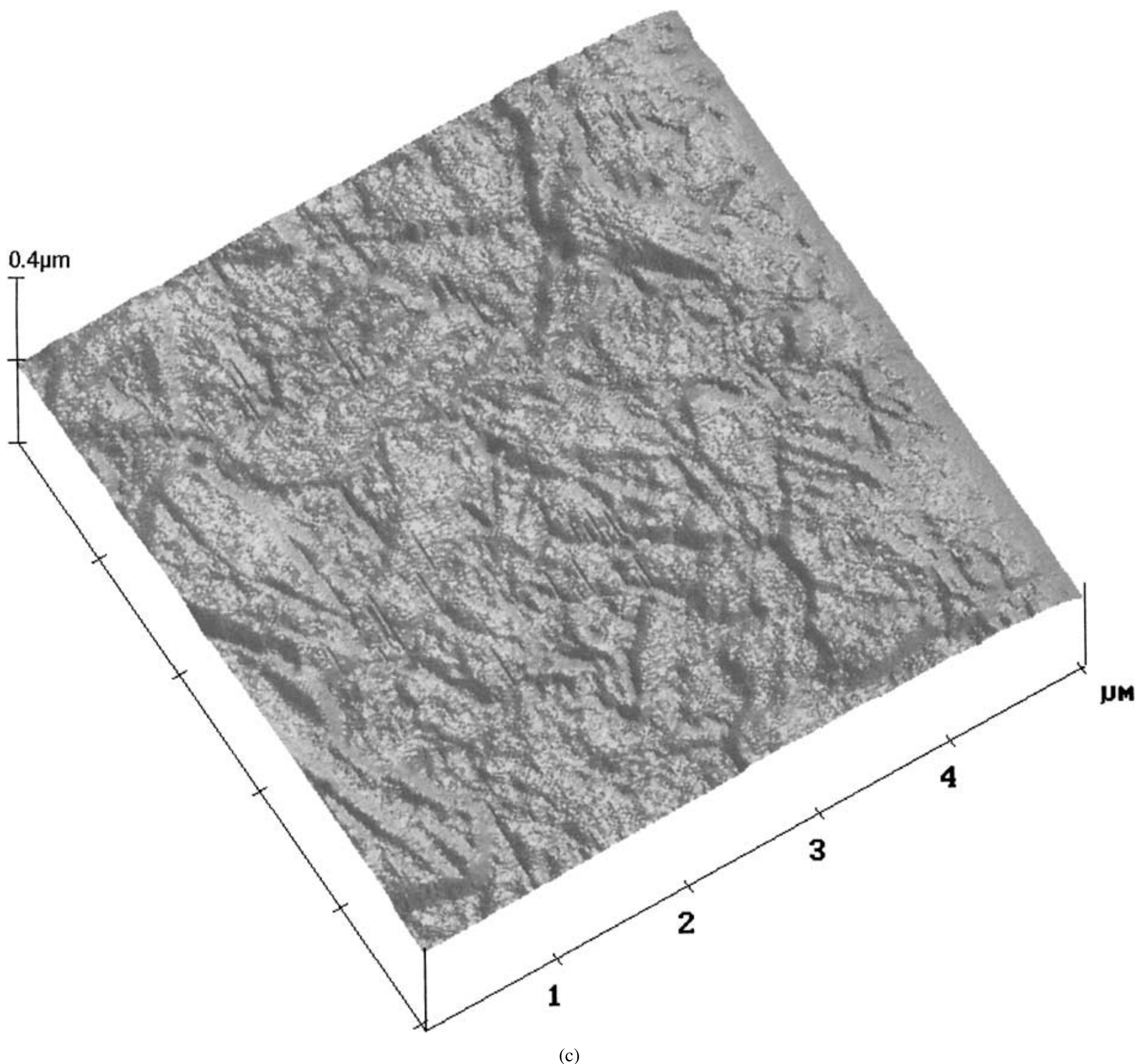

(c)

Figure 4 (Continued).

(d)

Figure 4 (*Continued*).

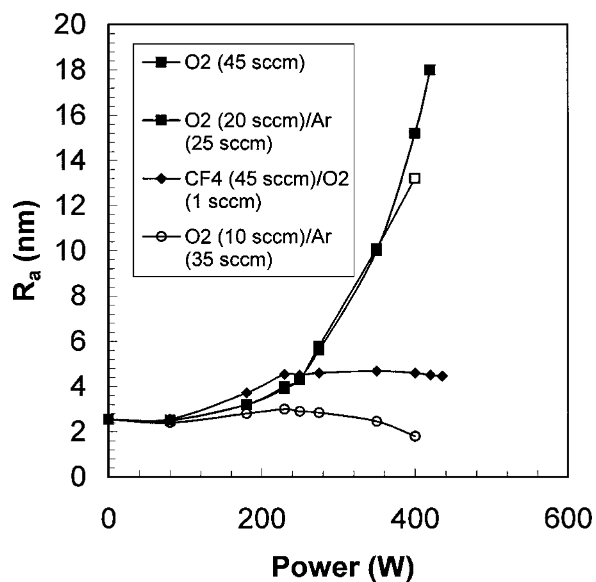

Figure 5 R_a (Average roughness) of the etched surfaces plotted as a function of power.

previously been shown to comprise an increased partial graphitisation as a result of bombardment by energetic ions [8].

In the O_2/Ar compositions, the continuous rise in the etch rate with proportion of O_2 has indicated a combination of the two processes. An increasing flow rate of O_2 evidently had the effect of an increasing the density of ions available for the ion-enhanced etch process relative to physical sputtering. This interpretation was supported by the trend of an increasing etch rate with flow rate in Fig. 3. The etch rate in the CHF_3/O_2 plasmas has similarly indicated a regime of sputter etching as with Ar. However, the larger value of slope constant, A, in CHF_3/O_2 than for Ar indicates that reactive etching was present in these plasmas. The CHF_3/O_2 plasmas have evidently provided a source of F and C but with a lower ratio of F/C than in CF_4/O_2.

4. Conclusions

The reactive ion etching of CVD diamond film in CF_4/O_2, O_2 and O_2/Ar plasmas (with a flow ratio of O_2/Ar $\geq$25%) has been attributed to a process of ion-enhanced chemical etching. In these plasmas, the etch rate and the slope constant (etch rate versus $V^{1/2}$), A, were comparatively high with a dependence on the flow rate. The roughness of the etched surfaces in the O_2 rich plasmas increased significantly with RF power while the CF_4/O_2 plasmas produced only a minor roughening at all power levels. For the diamond film etched in Ar plasmas, the low etch rates, the low value of the

constant, A, and independence of flow rate have indicated a regime of physical sputtering. This process, which was evident in Ar and Ar (35 sccm)/O_2 (10 sccm) plasmas, has produced a smoothing of the original surface but at a significantly slower rate of etching (7–9 nm/min) than in the O_2 (35 nm/min at 400 W) or CF_4/O_2 plasmas (50 nm/min at 400 W).

References

1. J. T. GLASS, B. A. FOX, D. L. DRIEFUS and B. R. STONER, *MRS Bulletin* **23** (1998) 49.
2. M. N. ASHFOLD and P. W. MAY, *Chemistry and Industry* (London) **13** (1997) 505.
3. G. B. SANDHU and W. K. CHU, *Appl. Phys. Lett.* **55**(5) (1989) 437.
4. A. VESCAN, W. EBERT, T. H. BORST and E. KOHN, *Diamond and Related Materials* **5** (1996) 774.
5. O. M. KUTTEL, L. DIEDERICH, E. SCHALLER, O. CARNAL and L. SCHAPBACH, *Surface Science* **337** (1995) 812.
6. C. VIVENSANG, L. FERLAZZO-MANIN, M. V. RAVET, G. TURBAN, F. ROSSEAUX and A. GICQUEL, *Diamond and Related Materials* **5** (1996) 840.
7. O. DORSCH, M. WERNER, E. OBERMEIER, R. E. HARPER, C. JOHNSTON and I. M. BUCKLEY-GOLDER, *ibid.* **1** (1992) 277.
8. W. J. ZHANG, C. SUN, I. BELLO, C. S. LEE and S. T. LEE, *JVST* **A17**(3) (1999) 763.
9. S. A. GROT, R. A. DITZIO, G. SH. GILDENBLAT, A. R. BADZIAN and S. J. FONASH, *Appl. Phys. Lett.* **61**(19) (1992) 2326.
10. K. KOBAYASHI, N. MUTSUKURA and Y. MACHI, *Thin Solid Films* **200** (1991) 139.
11. T. WHETTEN, A. ARMSTEAD, T. A. GRZYBOWISKI and A. L. RUOFF, *JVST* **A2**(2) (1984) 477.
12. N.N. EFREMOW, M. W. GEISS, D. C. FLANDERS, G. A. LINCOLN and N. P ECONOMOU, *ibid.* **B3** (1985) 416.
13. D. F. GROGAN, T. ZHAO, B. G. BOVARD and H. A. MACLEOD, *Applied Optics* **31**(10) (1992) 1483.
14. A. P. MALSHE, B. S. PARK, W. D. BROWN and H. A. NASEEM, *Diamond and Related Materials* **8** (1999) 1198.
15. H. OHASHI, E. ISHIGURO, T. SASANO and K. SHOBATAKE, *APL* **68**(26) (1996) 3173.
16. CH. STEINBRUCHEL, H. W. LEHMANN and K. FRICK, *J. Electrochem. Soc.* **132** (1985) 180.
17. CH. STEINBRUCHEL, *ibid.* **130** (1983) 648.
18. *Idem.*, *Appl. Phys. Lett.* **55**(19) (1989) 1960.
19. WILLIAMS and MULLER, *J. Microelectromechanical Systems* **5**(4) (1996) 258.
20. P. K. BACKMANN, D. LEERS and D. U. WIECHERT, *Diamond and Related Materials* **2** (1993) 683.

Received 24 May
and accepted 27 November 2000